Tectonophysics 490 (2010) 184–196

Contents lists available at ScienceDirect

Tectonophysics

journal homepage: www.elsevier.com/locate/tecto

Studies of Quaternary deformation zones through geomorphic and geophysical evidence
A case in the Precordillera Sur, Central Andes of Argentina

Carla M. Terrizzano [a,*], Sabrina Y. Fazzito [b], José M. Cortés [a], Augusto E. Rapalini [b]

[a] Consejo Nacional de Investigaciones Científicas y Técnicas (CONICET), Laboratorio de Neotectónica (LANEO), Departamento de Ciencias Geológicas, Facultad de Ciencias Exactas y Naturales, Universidad de Buenos Aires, Pabellón II, Ciudad Universitaria, C1428EHA, Buenos Aires, Argentina
[b] Consejo Nacional de Investigaciones Científicas y Técnicas (CONICET), Instituto de Geofísica Daniel Valencio (INGEODAV), Departamento de Ciencias Geológicas, Facultad de Ciencias Exactas y Naturales, Universidad de Buenos Aires, Pabellón II, Ciudad Universitaria, C1428EHA, Buenos Aires, Argentina

ARTICLE INFO

Article history:
Received 4 March 2009
Received in revised form 4 May 2010
Accepted 13 May 2010
Available online 23 May 2010

Keywords:
Neotectonics
Tectonic geomorphology
Tomography of electrical resistivity
Paleotectonic controls
Central Andes
Argentina

ABSTRACT

At the northern sector of the Precordillera Sur (31° 50′–32° 40′ SL/68° 45′–69° 20′ WL), Central Andes of Argentina, NW-trending sinistral transpressive shear zones at different scales, product of the Late Cenozoic Andean deformation, are recognized. The most significant of them is the 120 km long Barreal–Las Peñas Belt and within it, a small-scale (7 km long) Quaternary sinistral transpressive shear zone, called Los Avestruces, has been detected from geomorphological and geophysical analysis (32° SL/69° 21 WL). Geophysical techniques were applied to better characterize the shallow structure and kinematics of some representative structures in this shear zone. In particular, the use of tomography of electrical resistivity methods allowed characterizing the subsurface geometry of some areas of interest, enabling the recognition of Quaternary layers against their original slope, the geometry of the reverse fault which uplifted the Pleistocene deposits of one of the highs, the geometry of a likely previous extensional fault reactivated and inverted during the Quaternary as well as the presence of a reverse blind fault, which has uplifted the Quaternary deposits of the Los Avestruces bog.

The location of the above mentioned shear zones coincides with the northern branch of the NW-trending extensional Triassic Cuyana basin. Thus, their presence appears to be related to Andean reactivation of older (Triassic), mainly NW-trending, structures. In the northern area of the Precordillera Sur, as well as in other places of the world here discussed, these kinds of paleotectonic oblique features play a major role in defining the geometry and kinematics of Late Cenozoic deformation.

1. Introduction

Most of the evidence for Quaternary deformation along the Precordillera of Western Argentina is concentrated in its eastern edge (Costa et al., 2000, 2006; Fig. 1a). Nevertheless, the western edge, which has been much less studied, also shows evidence of Quaternary deformation. The nature, geometry and kinematics of this deformation are poorly known. Particularly, the neotectonic activity in the Precordillera (beyond its eastern limit) appears to be concentrated along a 120 km long oblique belt, called Barreal–Las Peñas, which extends from the Barreal block, in the Western Precordillera, to Las Peñas range in the Eastern Precordillera (Fig. 1a) to form what has been interpreted as a Late Cenozoic to Quaternary, first order left-lateral transpressive shear zone (Cortés et al., 2005a,b; Terrizzano et al., 2007).

The Barreal–Las Peñas belt is constituted by five NNW-trending ranges arranged in a left-stepping pattern (Fig. 1b), in marked contrast with the northwards arrangement of the Precordillera, characterized by over 150 km long, N–S trending parallel ranges and intermountain basins. It has been suggested that the distinctive behaviour of this southern region of the Precordillera could be related to Cenozoic to Quaternary reactivation of older structures (Cortés et al., 2005b) such as those associated with the Late Palaeozoic Sanrafaelic compressive event (Azcuy and Caminos, 1987; Mpodozis and Kay, 1990) and/or to the development of the extensional Triassic Cuyana basin (Strelkov and Álvarez, 1984; Uliana et al., 1989).

The well developed pattern of left-lateral transpressive zones is repeated at different scales within the Barreal–Las Peñas belt. This can be observed in the Barreal–Uspallata valley, at the piedmont area of the Ansilta and El Naranjo ranges, northwestern edge of the Barreal–Las Peñas belt (Fig. 1a,b). There, the soft-linked Yalguaraz belt

* Corresponding author. Tel./fax: +54 11 47883439x38.
E-mail addresses: cterrizzano@gl.fcen.uba.ar (C.M. Terrizzano), sabrinafazzito@gl.fcen.uba.ar (S.Y. Fazzito), cortes@gl.fcen.uba.ar (J.M. Cortés), rapalini@gl.fcen.uba.ar (A.E. Rapalini).

0040-1951/$ – see front matter © 2010 Elsevier B.V. All rights reserved.
doi:10.1016/j.tecto.2010.05.006

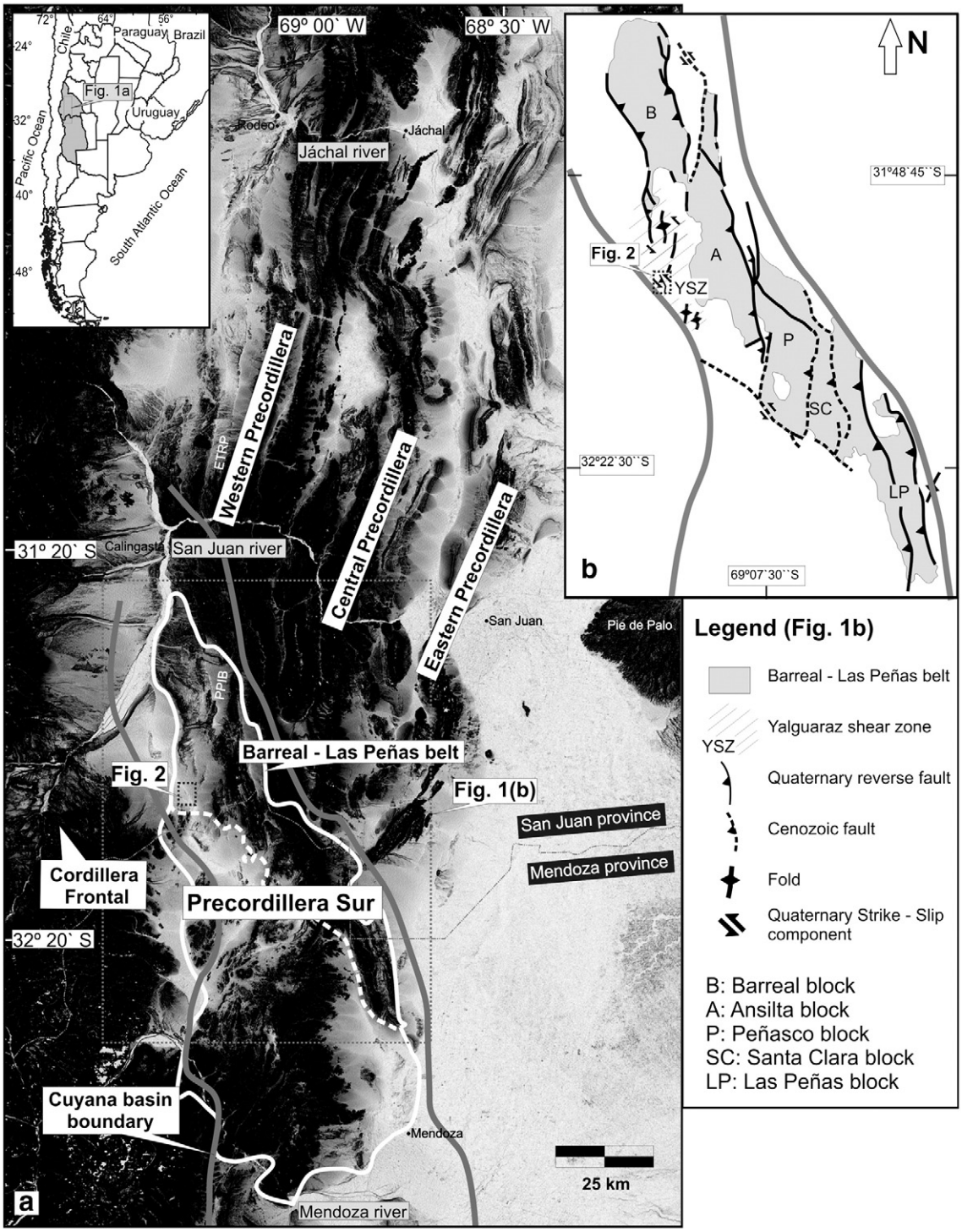

Fig. 1. a. Location of the morphotectonic units of Precordillera, Precordillera Sur and Cordillera Frontal on a Digital Elevation Model shaded relief. Full-white line indicates the Precordillera Sur boundary and the dot–black line its northern sector, the Barreal–Las Peñas belt. The gray lines indicate the Cuyana basin Triassic boundaries; ETRP: piedmont area of the El Tigre range; PPIB: Pampa del Peñasco intermountain basin. b. The Barreal–Las Peñas belt: a first order left-stepping transpressive shear belt. B: Barreal block; A: Ansilta block; P: Peñasco block; SC: Santa Clara block; and LP: Las Peñas block.

(Terrizzano and Cortés, 2008) and the Los Avestruces shear zone constitute examples of such Quaternary deformation zones.

Los Avestruces deformation zone is a 7 km long, oblique left-lateral transpressive shear zone, comprising a set of neotectonic structural highs. It is the smallest recognized Quaternary transpressive zone within the Barreal–Las Peñas belt, which due to its dimensions make it ideal for the study of these kinds of shear zones.

At the southeastern tip of this set of structures and due to the uplift of the southernmost structural high, the Los Avestruces bog was developed (Fig. 2). This is located to the east of the latter deformation zone, and it would be a consequence of tectonic damming of alluvial streams along the Precordillera piedmont (Fig. 2). The bog sediments also show evidence of deformation. The aim of this contribution is to characterize the structural and kinematical features of the Late Cenozoic to Quaternary Los Avestruces deformation zone and their relation with the regional structural framework. The sediments which are preserved uplifted at the top of structural highs, correspond to coarse-grained alluvial deposits. This kind of sediments does not

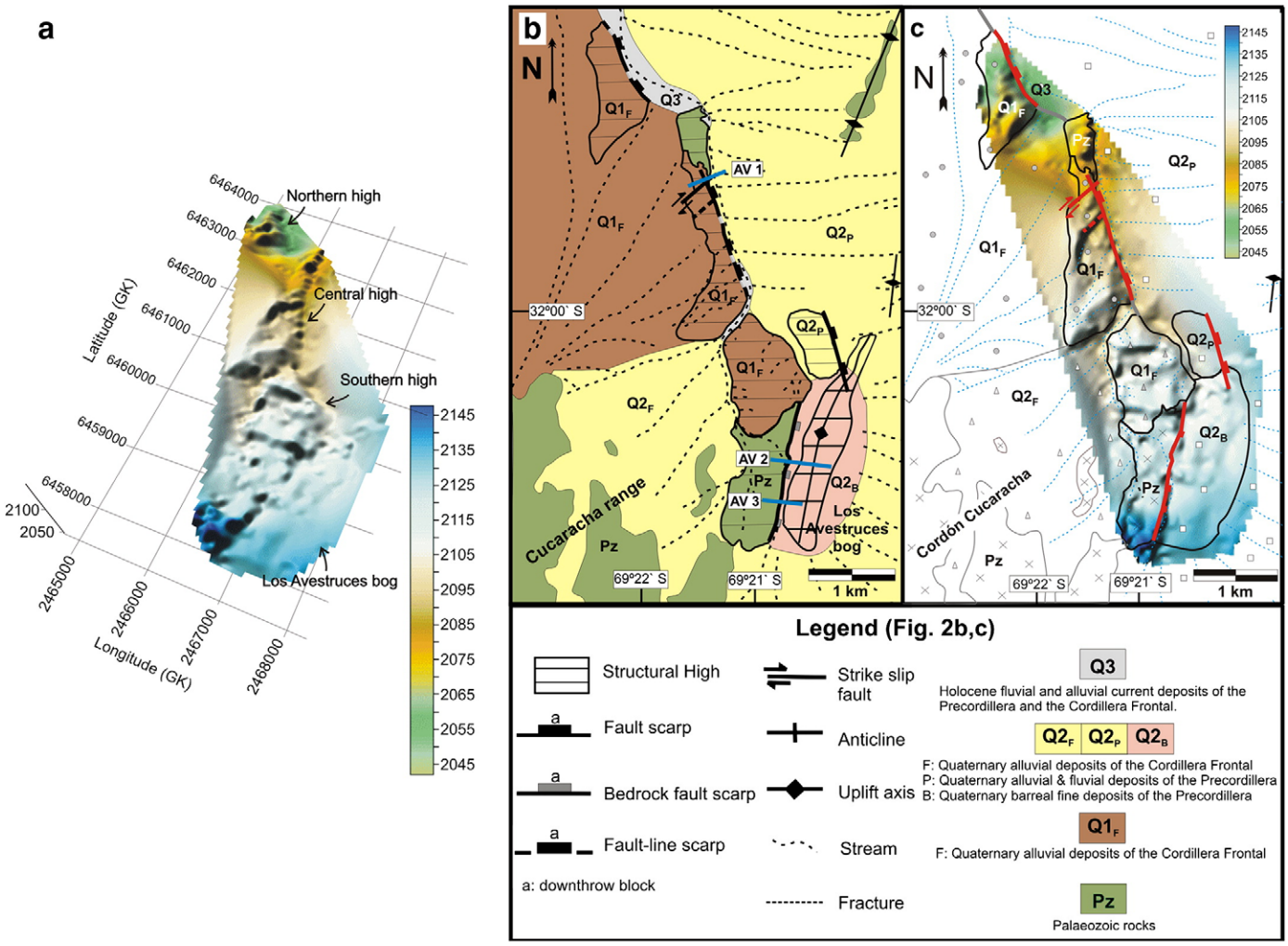

Fig. 2. a. Topographic map of the Los Avestruces deformation zone. It was carried out by a GPS navigator and a 0.5 m precision altimeter. It is possible to observe the left-stepping arrangement of the highs, their abrupt eastern edges, which we assume as tectonic, and a subtle topographic relief in the Los Avestruces bog area. b. An interpreted geological and structural sketch of the Los Avestruces deformation zone. Blue lines show the tomography of electrical resistivity traces. c. The same sketch redrawn over the topographic map.

favour the preservation of microtectonic kinematic indicators, such as slickenside lineations. In fact, the scarps that bound the structural highs show no microtectonic kinematic indicators. Furthermore, dip of the sedimentary layers along this zone cannot be determined from field observations. Therefore, our analysis followed two main lines of evidence: i) geomorphological and ii) geophysical. The latter was carried out by means of three cross-sections of tomography of electric resistivity (Telford et al., 1990) across the Los Avestruces deformation zone, with the purpose of getting information about the geometry of subsurface layers and structures. Two of these profiles cut across the Los Avestruces bog, in order to evaluate whether the Quaternary bog deposits have experienced tectonic deformation.

2. Tectonic framework

The Los Avestruces zone lies on the Central Andes of Argentina. The Central Andes ranges (including the Precordillera) have been developed during the latest orogenic cycle (Andean orogenic cycle) in Neogene times. However, at least two compressional and one extensional pre-Neogene events have conditioned the structural grain of the basement. The major pre-Andean deformation events in the study region include: 1) compressive Early to Middle Palaeozoic deformation (Devonian, Chañic phase, Ramos et al., 1984, 1986), 2) compressive Late Palaeozoic deformation (Lower Permian, San Rafael phase, Ramos and Ramos, 1979), 3) Late Permian to Triassic extension (Choiyoi magmatic cycle and Cuyana basin development, Strelkov and Álvarez, 1984).

The Middle to Late Devonian Chanic phase was a consequence of crustal shortening allegedly related to the collision of the allochthonous Chilenia terrane (Ramos et al., 1984, 1986) against the Gondwana margin. This event is represented by west-verging NW- to NE-trending metamorphic foliation in the Early Palaeozoic basement (Von Gosen, 1995).

Evidence of the Early Permian San Rafael phase (Ramos and Ramos, 1979) in the southern region of the Precordillera (Von Gosen, 1995; Cortés et al., 1997, 1999a,b) includes large- scale N–S to NNE–SSW trending folds and thrusts and NW-trending strike–slip faults (Von Gosen, 1995; Cortés et al., 1997). The San Rafael deformation phase has been widely documented along the Central Argentine Andes, at the Bloque de San Rafael (Azcuy and Caminos, 1987; Japas and Kleiman, 2004), the Cordilleras Frontal and Principal (Ramos, 1988; Llambías et al., 1993), as well as at the Barreal region in the northwestern edge of the southern Precordillera (Furqué and Cuerda, 1984). The wide distribution of this contractional event suggests that it resulted from a major change in the subduction regime along the western margin of Gondwana (Ramos et al., 1984; Ramos, 1988).

After a widespread extensional magmatic cycle (Choiyoi cycle), mostly developed during middle to late Permian times, a Triassic extensional phase produced widely scattered NNW-trending rift basins all over the western margin of Gondwana (Uliana et al., 1989). The Barreal–Las Peñas belt matches up with the northern end of one of these Triassic rift basins, the so called Cuyana basin (Strelkov and Álvarez, 1984, Fig. 1). Strelkov and Alvarez's (1984) maps show a NNW striking Cuyana basin with NNW to NW and NNE to NE trending normal faults. Meso and microscopic kinematic indicators in the southern sector of the Precordillera suggest a NE direction of extension with a sinistral shear component during this extensional event (Cortés et al., 2008; Japas et al., 2008).

The Neogene and Quaternary deformations are related to the Andean contractional orogenic cycle (Dewey and Lamb, 1992). In the Central Andes, the evolution of the flat slab subduction since the Miocene and the crustal anisotropies have conditioned the Late Cenozoic development of morphotectonic units during the last 15 Ma. Particularly, in the southern region of the Precordillera, several authors have interpreted the Andean contractional deformation to be associated with inversion of the extensional structures that developed the Cuyana basin (Ramos and Kay, 1991; Kozlowski et al., 1993; Legarreta et al., 1993; Cortés et al., 1997).

Oblique Palaeozoic deformation zones in the southern Precordillera have been reactivated during Triassic (Cortés et al., 1997; Giambiagi and Martínez, 2008) and Neogene times (Cortés, 1998). The inherited structures have probably played an important role in the geometry and kinematics of the Neogene to Recent deformation and the consequent morphotectonic segmentation of the Precordilleran ranges. The Precordillera was considered previously as a unique morphotectonic unit with a single geologic history. However, it has been observed that its deformation style changes laterally (Ortiz and Zambrano, 1981; Baldis et al., 1982). Whereas in the central region of the Precordillera, where the Lower Permian structures (San Rafael phase) and Triassic extensional faults of Cuyana basin are absent, the Late Cenozoic contractional deformation under slightly oblique convergence (Az 80°–85°) between the Nazca and the South American plates has built an east-verging thin-skinned belt with a general N–S trend of thrust sheets and intermontane basins, the southern region shows evidence of tectonic inversion of the Cuyana basin (Ramos and Kay, 1991; Kozlowski et al., 1993; Legarreta et al., 1993; Cortés et al., 1997, 2005a). Distinctive features of the southern region of the Precordillera (in contrast with the central region), such as its different structural style and morphotectonic design were used by Cortés et al. (2005a) to define a new morphotectonic unit called the Precordillera Sur (Fig. 1). According to these authors, the Precordillera Sur is characterized by shorter NNW to NNE blocks, up to 30 km length, limited by high-angle reverse faults which sometimes are associated with oblique (NW) and transverse (WNW) strike–slip structures. These oblique and transverse structures are recognized as a distinctive feature (Cortés et al., 2005b) which controls the end and subsequently the segmentation of the mountain fronts.

3. Tectonic geomorphology and Quaternary structural elements of the Los Avestruces highs

A group of 1 to 2.5 km long, NNW-trending Quaternary to Recent structural highs has been recognized in the Pleistocene sedimentary cover at the northwestern sector of the Barreal-Las Peñas deformation belt (Figs. 1b, 2). Their relief can only be properly characterized by appropriate scale topographic maps. We have made a detailed topographic map, by a survey with a GPS navigator and a high resolution altimeter, in order to characterize the shape and the distribution of the structural relief over the alluvial surface, showing its characteristics beyond their subtle surficial expression (Fig. 2a).

The highs, which were carved by the uplift and tilting of a set of alluvial fan deposits, are located in the Barreal–Uspallata tectonic depression between the morphostructural units of the Precordillera (to the east) and the Cordillera Frontal (to the west). The presence of three distinctive highs has been found: a northern, a central and a southern one. They are 20–30 m height and constitute a 7 km long, NW-trending zone which has a left-stepping arrangement (Fig. 2). Therefore, these left-stepped structural highs define a narrow and small structure called Los Avestruces deformation zone (Terrizzano et al., 2007). These small-scale features are also partially recognizable at aerial photographs and in the field (Fig. 3).

The sediments which form the alluvial fans are sourced in the Cordillera Frontal ranges to the west as well as in the Precordillera ranges to the east. Based on the cut and fill relations, the continuity and the different altitudes of the aggradation levels, three Quaternary alluvial and fluvial deposits of different relative age could be recognized: Q1, Q2 and Q3, where Q1 is the oldest and Q3 the youngest.

Two Quaternary alluvial deposits come from the Cordillera Frontal ranges (Fig. 2b), an older one called Q1F and a younger one called Q2F. On the other hand, the Q2P alluvial deposits as well as the Los Avestruces bog sediments (Q2B, Fig. 2c) come from the Precordillera ranges.

Although there are no absolute ages for these deposits, it is possible to assign some tentative chronologic constraints by correlating them with a set of alluvial deposits located 100 km farther north, at the piedmont area of the El Tigre range (ETRP in Fig. 1a). There, different aggradation and erosion levels were dated with cosmogenic nuclides (^{10}Be) by Siame et al. (1997a,b) and Siame (1998). A first correlation was made by Yamín (2007) for the alluvial deposits of the Pampa del Peñasco intermountain basin (35 km northwards from the Los Avestruces zone, PPIB in Fig. 1a). Yamín (2007) demonstrated the continuity of different aggradation levels in the neighbouring intermountain basins of the Precordillera to the north, and related their regional persistence with a climatic origin. Since the aggradation levels studied by Yamín (2007) continue in our study zone, we can extend this correlation in order to assign preliminary ages to the aggradation levels in the Los Avestruces zone.

Thereby, the ages of the Q1 and the Q2 alluvial deposits may range between 670 ± 140 ka to 580 ± 120 ka (Middle to Lower Pleistocene) and 380 ± 78 ka to 21 ± 4 ka (Middle to Upper Pleistocene), respectively. Finally, Q3 correspond to the current alluvial and fluvial deposits (Holocene).

The northern and the central highs are bounded by NW and NNW-trending fault-line scarps respectively, which cut the Palaeozoic substratum as well as the oldest Quaternary alluvial deposit (Q1F, Fig. 2b). Although they are partially eroded by active streams, these fault-line scarps were defined as such because they have a rectilinear path and bound structural highs. The Central high is cut also by other NE trending right-lateral fault and farther to the east a younger alluvial deposit (Q2P) is affected by a NNW-east facing-fault scarp. The southern high is limited by a NNE bedrock fault scarp, which affects the Palaeozoic substratum and interferes with the above mentioned NNW faults (Fig. 2b). This NNE-trending fault has a reverse behaviour farther south, where it bounds the Cucaracha range.

Close to the southern high and to the east lies the Los Avestruces bog, which may also be uplifted. The NNW-trending piedmont scarp that cuts the Q2P level (the one we have integrated into the Southern high) seems to affect the bog deposits (Q2B). From analyses of aerial photographs and the detailed topographic map, it is possible to elucidate some gently but clearly elevated areas, particularly a narrow vaulted NNE-trending one that involves the Quaternary bog deposits (Fig. 2a,c).

The fine bog sediments were likely deposited as a consequence of tectonic damming of alluvial streams on the Precordillera piedmont since the Quaternary uplift of the southern high, which apparently works as an obstacle to the drainage in that area. Thus, based on the evidence for Quaternary deformation in this area, it would be reasonable to suspect a tectonic genesis for the vaulted bog deposit. Additionally, if

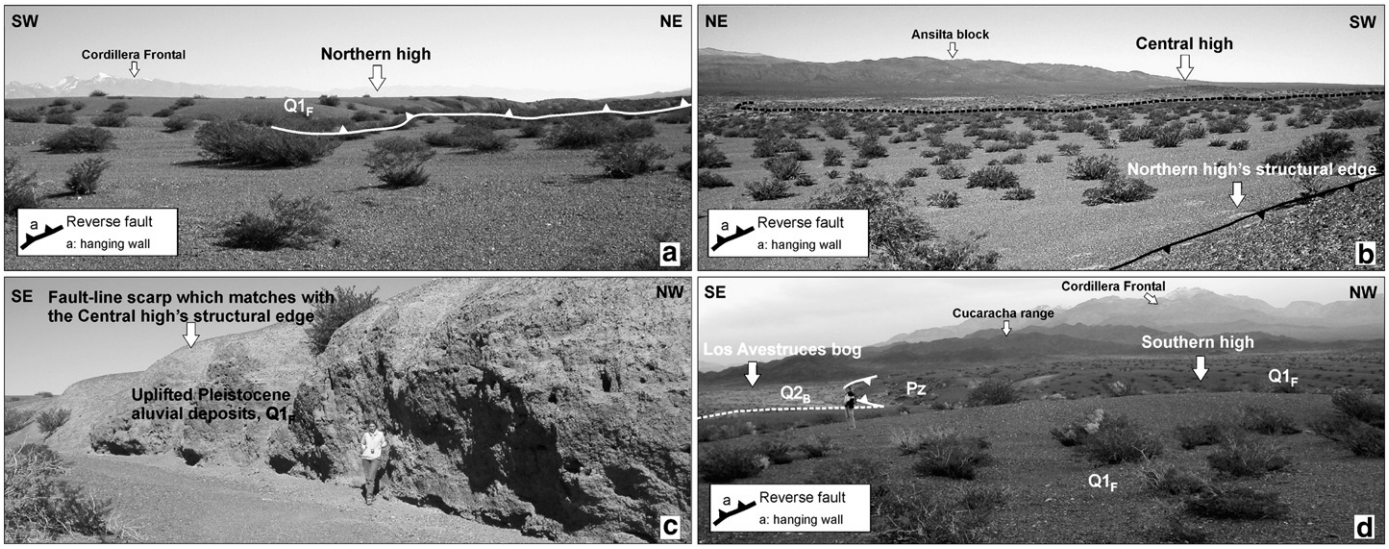

Fig. 3. Field views of the Northern, Central and Southern structural highs and of the Los Avestruces bog. a. Structural boundary of the northern high interpreted as a reverse, east-verging, fault which uplifted and tilted the Pleistocene alluvial sediments of Cordillera Frontal ($Q1_F$). b. Structural boundary of the Northern high (bottom–right) and the western side of the Central high (dot line). c. Pleistocene alluvial deposits of Cordillera Frontal in a view of the eastern edge of the Central high. d. Uplifted Palaeozoic outcrops and Pleistocene deposits of the Southern high. At the left, the Pleistocene strained? deposits of the Los Avestruces bog.

the development of the Los Avestruces bog is interpreted as caused by the Quaternary uplift of the southern high and the consequent stream damming and it has also been uplifted, it is possible to interpret at least two Quaternary deformation events related to displacements along the NNE border-fault of the southern high.

4. Tomography of electrical resistivity surveys

4.1. Electrode arrays and data acquisition

In order to obtain information about the subsurface geometry of the structures interpreted to have controlled the geomorphic features described above, a resistivity survey was carried out. Based on the survey, we have constructed three 2D tomographic profiles of electrical resistivity across the Los Avestruces highs. The *AV1* profile tomography crosscuts, from west to east, the westernmost edge of the Central structural high in Pleistocene deposits, a NNW-trending fault scarp facing east, a small outcrop of Palaeozoic clastic metasediments which bounds the Central high and finally, Quaternary alluvial deposits of the Precordillera (Q2P, Fig. 2b). The profile included the eastern edge of this ridge in order to decide whether it can be considered a structural boundary. The *AV2* and *AV3* profiles cut across the southern high, including a Palaeozoic outcrop and its eastern edge, given by a NNE fault scarp facing to the east, and the Los Avestruces bog, including the NNE-trending vaulted zone (Fig. 2b).

The resistivity survey aims at estimating the distribution of electrical resistivity in the subsurface. This, in turn, can be interpreted in terms of lithology, structure and fluid content. Application of this kind of surveys to map active faults has proved to be successful (e. g. Storz et al., 2000; Demanet et al., 2001; Caputo et al., 2003; Colella et al., 2004; Fazzito et al., 2006, 2009), although it has not yet been adopted as a standard practice in neotectonic studies. Areas with a high secondary porosity are frequently developed around active faults, allowing the increase of fluid content which is generally accompanied by a significant decrease in the electric resistivity. Sudden lithologic discontinuities due to the presence of a fault in the subsurface also are generally indicated in the tomography by sudden lateral changes in the resistivity patterns.

In this contribution, the main objectives of the resistivity surveys were: i) to get information about the geometry (dip direction and sense of movement) of the faults, in order to elucidate their normal or reverse character, ii) to associate the faults with the regional known Cenozoic structures as well as with the older ones (Palaeozoic and Triassic), since the study zone coincides with the extension in subsurface of the Triassic extensional Cuyana basin, old normal faults might have been inversely reactivated during the Andean contractional regime; iii) to get information on the structure of the substratum and the Pleistocene–Holocene layers of the Los Avestruces bog, in order to corroborate the extent of tectonic deformation of these deposits.

To perform the resistivity measurements along the three profiles a Syscal R1 Plus Switch 48 Georesistivity-meter (Iris Company) was employed. The electrodes are connected on the back of the resistivity-meter by means of two strings of heavy-duty seismic-like cable with 24 out-put each, conforming a linear array of 48 electrode nodes, with a 10 m of maximum spacing. A further extension to 72 or more electrodes can be done by applying the *roll along* technique. A sequence of measurements can be developed by setting acquisition parameters (maximum permitted standard deviation of the measurement, minimum and maximum numbers of stacks per measurement, current injection time per cycle and desired signal voltage) and geometric parameters (level n and electrode spacing d). The parameter n is sometimes called the dipole separation factor and is related to the pseudo-depth level. For example, if $C1$ and $C2$ are the current electrodes, and $P1$ and $P2$ are the potential electrodes, d is the length of the $C1$–$C2$ dipole or the $P1$–$P2$ dipole. The distance between the electrodes $C1$ and $P1$ is set to n *times* d, n being an integer or a fraction. The resistivity-meter is able to automatically perform the pre-defined sequence of measurements, according to the type of array selected, and provides direct reading of injected current, potential difference, electrode location and associated apparent. Geometric parameters n (level) and d (electrode spacing) are assigned according to the desired maximum depth of investigation, resolution and noise level.

Values of the acquisition and geometric parameters are a compromise between quality, duration of the survey and desired depth of investigation. Table 1 resumes the geometric and acquisition parameters chosen for each cross-section. For all of them, the dipole–dipole array was used because it has been shown to provide better imaging of high-angle faults (Loke, 1996–2009) and high lateral sensitivity (Coggon, 1973). Dahlin and Zhou (2004) have performed numerical simulation to study and compare the resolution, the image quality with different data densities and the sensitivity to noise levels of 2D resistivity imaging survey on typical geological and

Table 1
Geometric and acquisition parameters set for the design of the three dipole–dipole geoelectrical surveys.

Survey	Electrode spacing d [m]	Separation factor n	Total number of quadrupoles	Current injection time [S]	Profile length [m]	Stack minimum–maximum	Maximum standard deviation [%]
AV1	10	1 to 6 (integers)	545	1	470	2–6	5
	20	3 to 12 (integers)					
AV2	10	1 to 6 (integers)	1189	1	710	2–4	3
	20	3, 7/2, 4, 9/2, 5, 11/2, 6					
	30	4, 13/3, 14/3, 5, 16/3, 17/3, 6					
AV3	10	1 to 6 (integers)	689	1	470	2–4	3
	20	3, 7/2, 4, 9/2, 5, 11/2, 6					
	30	4, 13/3, 14/3, 5, 16/3, 17/3, 6					

environmental cases for standard arrays of 10 electrodes. The dipole–dipole array is among the arrangements that have better resolution images, despite that it is susceptible to noise contamination. Further successful application of the dipole–dipole array in imaging faults can be found in Fleta et al. (2000), Caputo et al. (2003), Rizzo et al. (2004), Fazzito et al. (2006, 2009), Nivière et al. (2008). Caputo et al., 2007 remarked that the resistivity patterns obtained with the Wenner–Schlumberger array are generally more flattened and thus impedes easy characterization of subvertical features and prefers the dipole–dipole array for imaging faults.

The graphical representation of the measurements is shown in the way of apparent resistivity pseudosections in Figs. 4a, 5a and 6a. A histogram of the apparent resistivity standard deviations σ during each measurement process of cross-sections AV1, AV2, AV3 are shown in Fig. 7. Total number and percentage of measurements with a standard deviation equal or minor than 2%, between 2 and 4% and so on are represented. It is evident that all three cross-sections have an overwhelming set of measurements with very low experimental errors ($\leq$2%) and no standard deviations greater than 24% was observed. This is significant considering that the dipole–dipole method generally suffers from very low potential values measured in the field. The data can therefore be considered of good quality. AV2 and AV3 show somewhat better results than AV1. The reason for this is the use of elevated number level n for $d=2$, which produces low signal at the reception. This feature is consistent with the recommendation (see for example Loke, 1996–2009) of not using the level number n greater than 6 (or sometimes 4). Instead, it is proposed to increase the spacing number d (and use fractional numbers for n) in order to reach deeper exploration depths. In this sense, AV2 and AV3 surveys have better quality data and we encourage these types of geometrical configurations for the future in order to reduce the noise.

Largest standard deviations (σ>6%) are registered only when the signal is too weak (<25 mV), however not all the measurements with low signal has higher standard deviation. Measurements with best quality (σ<6%) include signals in the range 25 mV–360 mV. Apparent resistivity measurements with standard deviation >10% were ruled out and a few anomalous apparent resistivity values have been discarded.

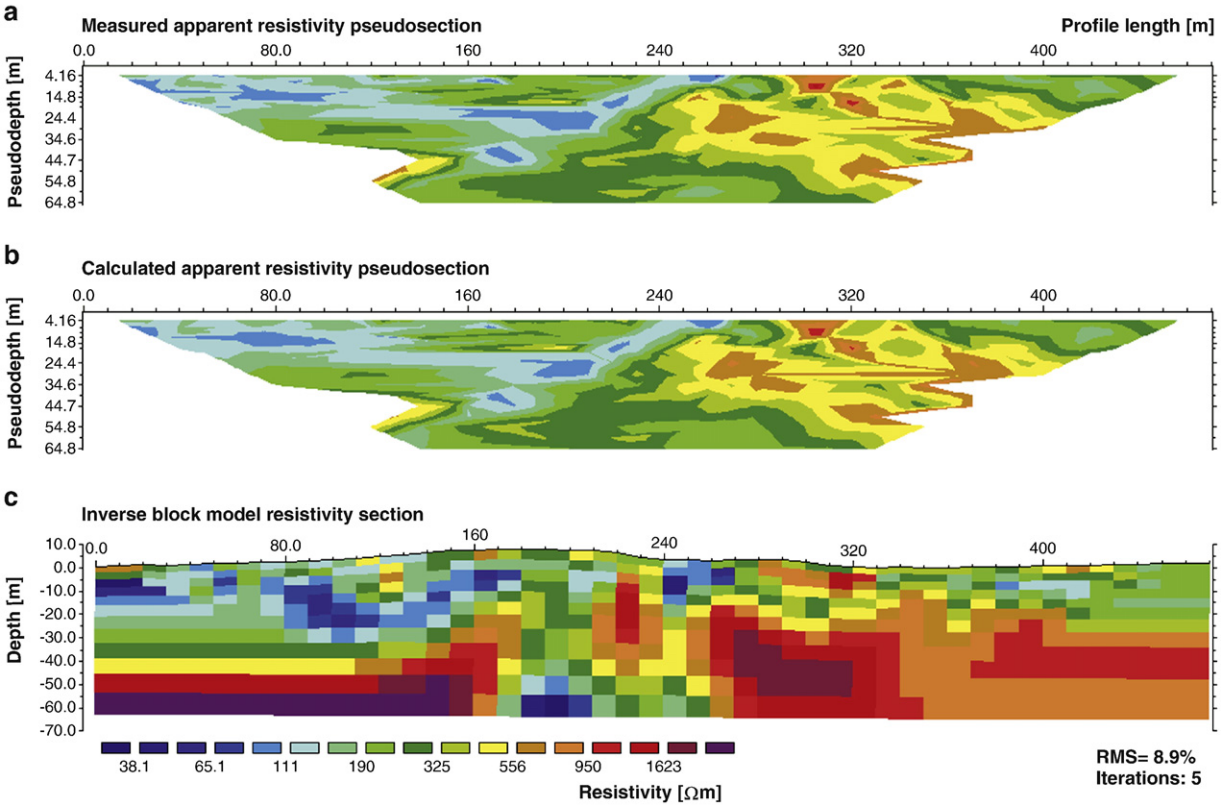

Fig. 4. a. Apparent resistivity pseudosection from field measurements for AV1 cross-section through the Los Avestruces Central high (dipole–dipole array, unit electrode spacing of 10 m) b. Calculated apparent resistivity pseudosection. c. Block model section where the maximum penetration depth was 60 m.

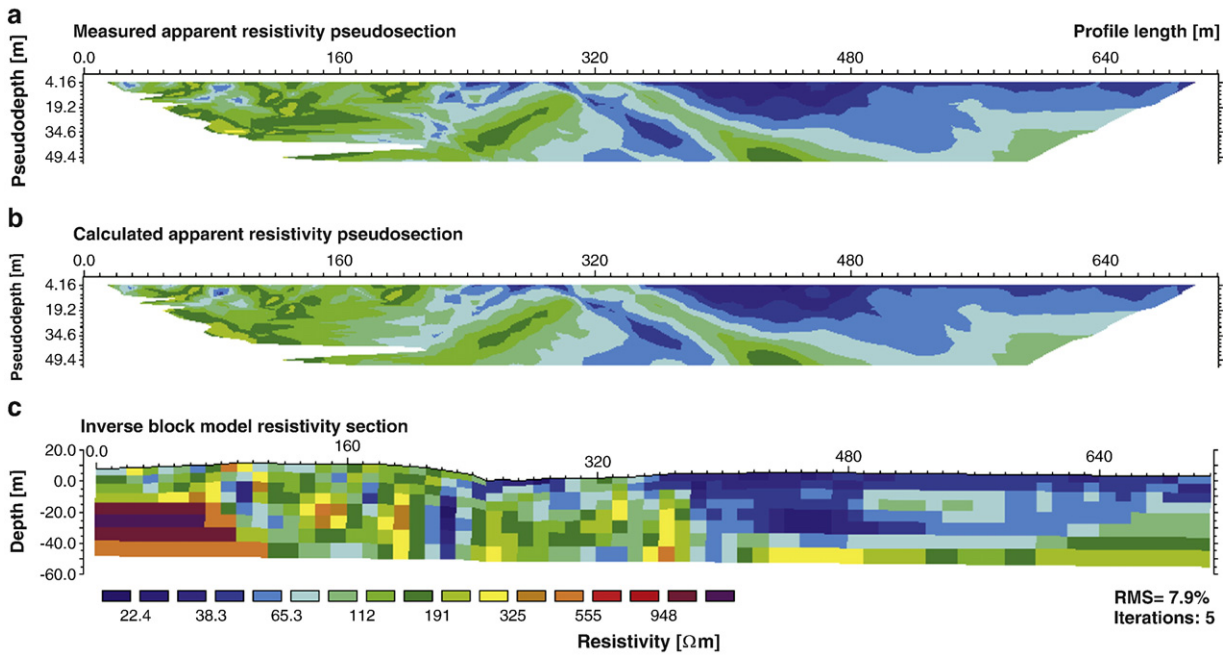

Fig. 5. a. Apparent resistivity pseudosection from field measurements for AV2 cross-section through the Los Avestruces Southern high (dipole–dipole array, unit electrode spacing of 10 m) b. Calculated apparent resistivity pseudosection. c. Block model section where the maximum penetration depth was 50 m.

4.2. Resistivity imaging

The process of geophysical inversion involves the estimation of the parameters (resistivities) of a postulated earth model from a set of observations (Lines and Treitel, 1984). The problem of finding an inverse 2D model of resistivity distribution in a profile was solved numerically in the form of a simple rectangular cell model by means of the RES2DINV software, of Geotomo Software (Lines and Treitel,

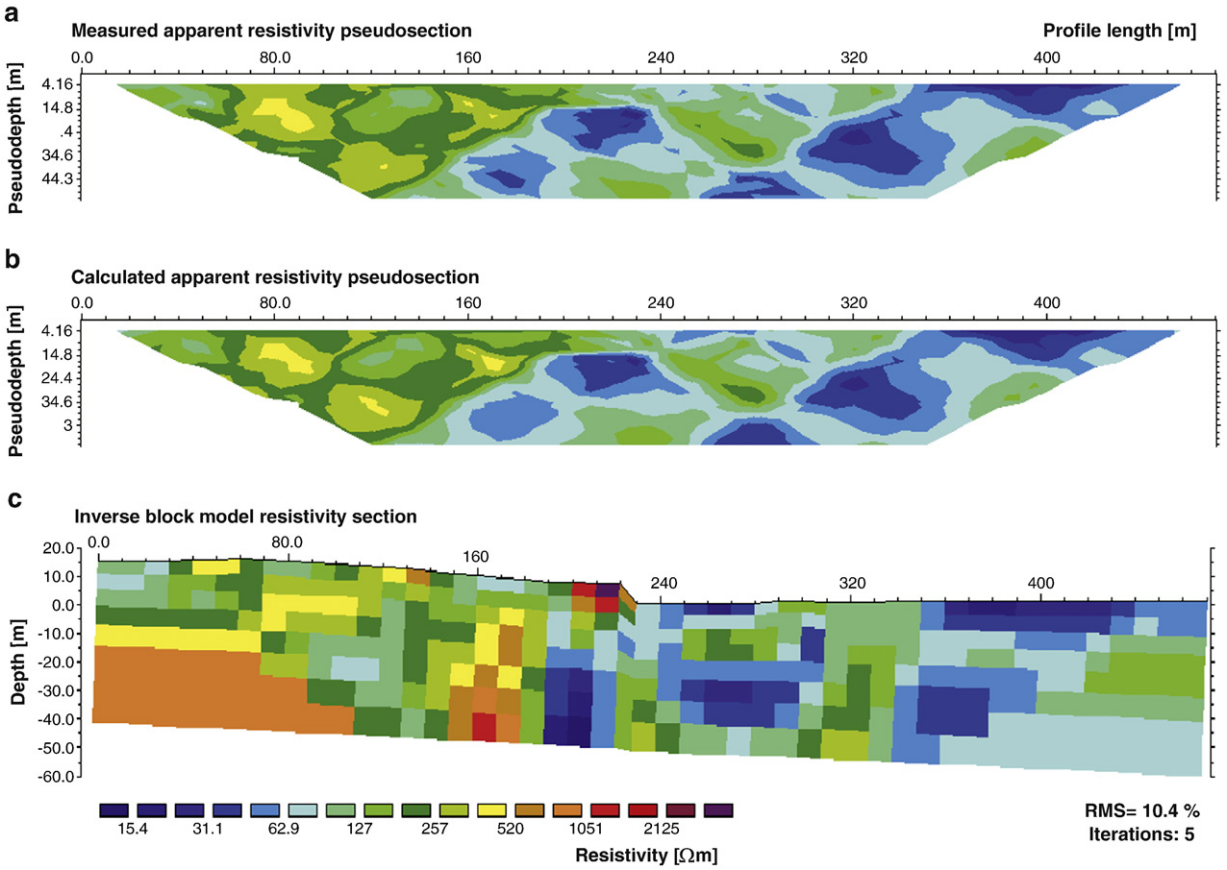

Fig. 6. a. Apparent resistivity pseudosection from field measurements for AV3 cross-section through the Los Avestruces Southern high (dipole–dipole array, unit electrode spacing of 10 m) b. Calculated apparent resistivity pseudosection. c. Block model section where the maximum penetration depth was 50 m.

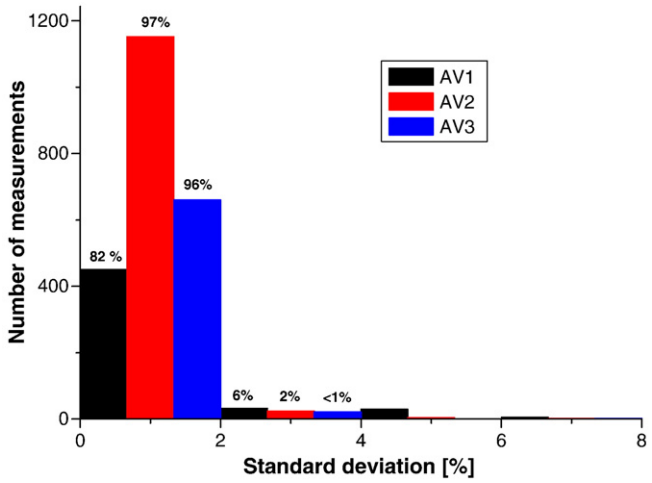

Fig. 7. Histogram of the standard deviation of the apparent resistivity measurements for the three surveys.

1984; Loke, 1996–2009; Loke, 2001). With this software it is possible to estimate the resistivity of the cells (model parameters) that adjusts the quantities measured at surface, within certain discrepancy. At first, the quantities derived from the field measurements are presented in the form of a *pseudosection*, a contour diagram in which the *apparent resistivity* values are assigned to a pre-defined location according to the array type used and setting of the geometric parameters (Telford et al., 1990). During the inversion routine the initial model parameters are modified and improved by solving a least-squares equation. This Gauss–Newton equation determines the corresponding change in the model parameters that should reduce the sum of squares of the discrepancies between the logarithm of the apparent resistivity values calculated from the cell model and the logarithm of the apparent resistivity values deduced from the real field data, and also minimizes the change in the model parameters between iterations (smoothness-constrained least-squares method). The discrepancy between the calculated values of apparent resistivity and those inferred from the field data are expressed through the root mean square (RMS). A modification can also be introduced in the optimization algorithm which consists in minimizing the sum of squares of the spatial changes in the model parameters (smoothness-constrained least-squares method with smoothing of model resistivity), thus the model resistivity values in the section change in a smooth manner. An alternative optimization method is the *blocky inversion*, in which the quantity to be reduced is the sum of absolute values of the discrepancies. In this case, a final model with sharp boundaries and homogeneous resistivity distribution within the bodies is expected (robust modelling alternative). These methods of regularization (where additional information is incorporated), are used in order to reduce the non-uniqueness of the problem and stabilize the iterative inversion (Lines and Treitel, 1984). Finally, a contour diagram based in the resistivity distribution of the model constitutes the ERT.

In this work, we propose a solution of the geophysical problem based on previous experiences and diverse geological settings (Loke, 1996–2009; Fazzito et al., 2006, 2009). The forward modelling subroutine (calculus of apparent resistivity from resistivity model parameters) and Jacobian matrix calculation were executed both by finite-element method. For the inverse model, the smoothness-constrained least-squares method (reduction of l_2 norm) with smoothing of model resistivity values was generally used. Topography information in the cell model was incorporated by means of a distorted finite-element mesh: all nodes along the same vertical line are shifted the same amount according to the elevation of the ground surface (uniformly distorted grid). The investigation depths depended on the number n of levels chosen, the electrode separation, the total length of profiles and the type of array.

Figs. 4b, 5b and 6b present the calculated apparent resistivity pseudosection and Figs. 4c, 5c and 6c show the solutions of the geophysical problem in the form of block models. The block model is helpful to appreciate the resolution of the tomographies. The cell size was over imposed by the expected variation in spatial resolution of resistivity: the width of the cells were constrained by the minimum length of the dipoles (being 10 m for these surveys) and the depth of the cells reflect the fact that resolution decreases with depth (the thickness of each deeper layer was systematically increased by a moderate amount of 10%), i.e. the size of the objects that can be resolved, increase with depth as in all geophysical methods. In the case of AV1 the final model has 432 cells of equal width distributed in 12 layers. The maximum depth of the model is 60 m. This resistivity model reaches a RMS of 8.9% in 5 iterations. The second model AV2 has 489 cells of equal width in 8 layers. The RMS estimated in this case is 7.9% in 5 iterations. The maximum depth of the model is estimated in 50 m. The AV3 resistivity model has 298 cells of equal width within 8 layers and has a RMS of 10.4% in 5 iterations. The maximum depth of this model is estimated also in 50 m.

4.3. Results and interpretation

Considering the resistivity distribution of the selected models AV1, AV2 and AV3, typical tabulated resistivity values of rocks and alluvium, and association of electrical properties with information from exposed geological units, interpreted geological cross-sections were produced from each of these profiles. For straightforward elucidation, the interpretation is based on the contoured sections created from the respective block models shown in Figs. 8, 9 and 10.

Along the AV1 profile (Fig. 8), the scarp has a small topographic relief (less than 1 m) and is located at a distance of 220 m, showing an uplifted western block. The inverse model is consistent with the presence in the field of Quaternary alluvial fans beds ($\rho<325\ \Omega$ m) both to the west ($d<180$ m) and to the east ($d>330$ m) of the scarp. Beds on the western and on the eastern side apparently dip west and east respectively, opposing the regional and original slope and suggesting that the Quaternary infill has been tilted as a consequence of compressional deformation. This subtle geometrical feature in the resistivity model is interpreted as a real feature of the subsurface, and not an artefact of the contoured sections as it can also be recognized in the block model of Fig. 4c. A conspicuous resistivity discontinuity is evident in the subsurface coincident with the location of the scarp. This suggests that the scarp is associated with a west-dipping high-angle fault. Exposures of Palaeozoic rocks to the East of the scarp ($d=320$ m) and the corresponding high resistivity values permit to assign the high resistivity zones in the subsurface ($\rho>900\ \Omega$m) to these rocks. A significant throw of around 25 m is suggested by the resistivity distribution across the fault. Since the distribution of the Palaeozoic rocks indicates that the hanging western block is downthrown, it must be concluded that the fault worked as a normal fault after the Palaeozoic, most probably during the Triassic. This is opposite to the reverse movement indicated by the Quaternary sediments displaced along the scarp. Reconciliation of these observations is to interpret this fault as a reactivated extensional fault, originally associated with the development of the Triassic Cuyana basin but inverted in the Quaternary. The significantly larger older throw allowed us to depict the original normal character of the fault. The geophysical survey thus appears to provide confirmation on the small scale of Andean reactivation of Late Palaeozoic–Early Mesozoic structures (Cortés, 1998).

As a secondary observation, no evidence is shown by the electrical survey of a fault bounding the eastern limb of the Los Avestruces Central high.

Along the AV2 profile (Fig. 9), two contrasting resistivity zones, a western ($0<d<250$ m) and an eastern one ($250<d<710$ m), can be

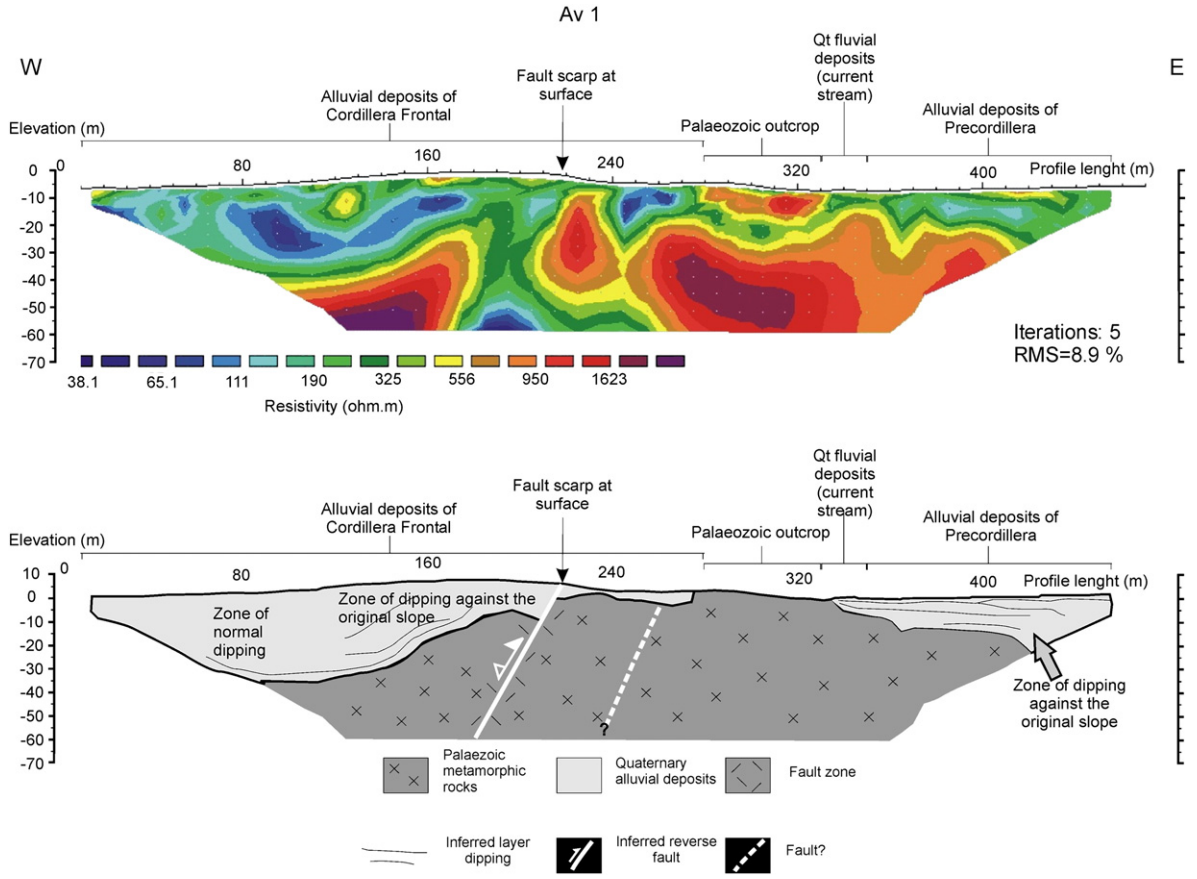

Fig. 8. Tomography of electrical resistivity AV1. a. Selected inverse model performed through the Los Avestruces Central high. A dipole–dipole array was used with a unit electrode spacing of 10 m. (Smooth-constrained inversion). Maximum penetration depth was 60 m. b. Interpreted geological cross-section.

observed. The whole western zone, which corresponds on the surface with the southern high Palaeozoic outcrops, has greater resistivity values ($100\ \Omega\ m<\rho<1850\ \Omega\ m$). A lower resistivity zone acts as a discontinuity that limits this western zone and coincides on the surface with the 4.5 m high east facing fault scarp that raised the southern high. Therefore, the discontinuity is interpreted as a west-dipping reverse fault.

Along the eastern zone, Palaeozoic outcrops ($d=320$ m) are consistent with a clear resistivity high located between the low resistivity

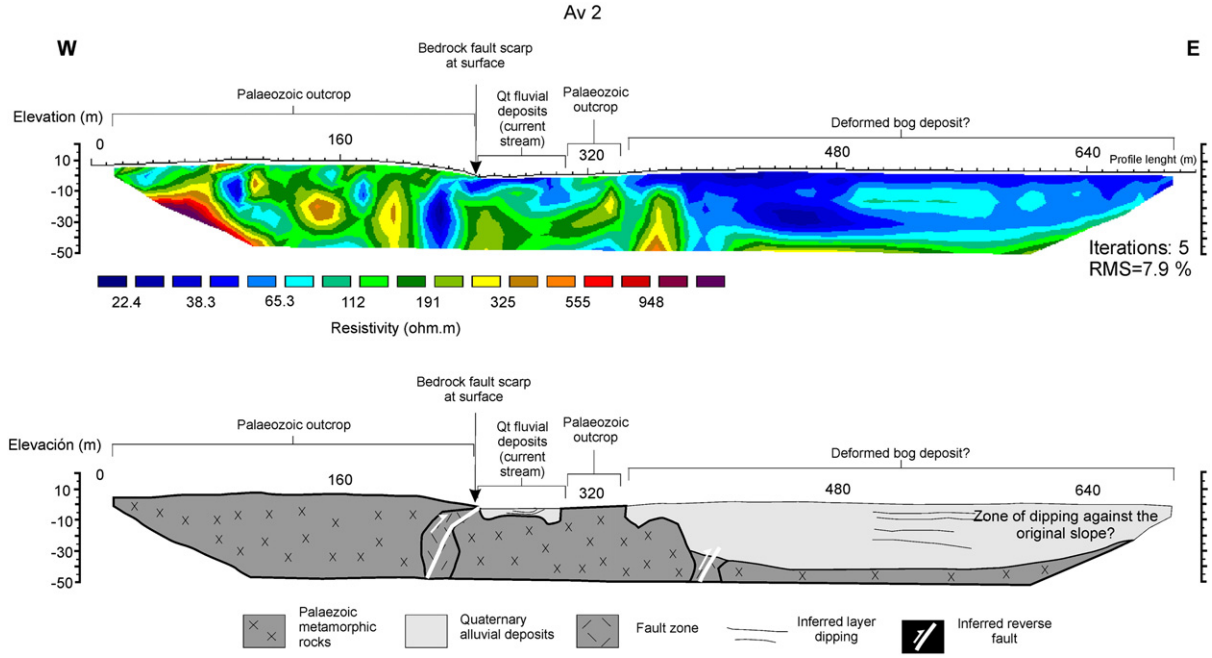

Fig. 9. Tomography of electrical resistivity AV2. a. Selected inverse model performed through the Los Avestruces Southern high. A dipole–dipole array was used with a unit electrode spacing of 10 m. (Smooth-constrained inversion with smoothing of model resistivity values). Maximum penetration depth was 50 m. b. Interpreted geological cross-section.

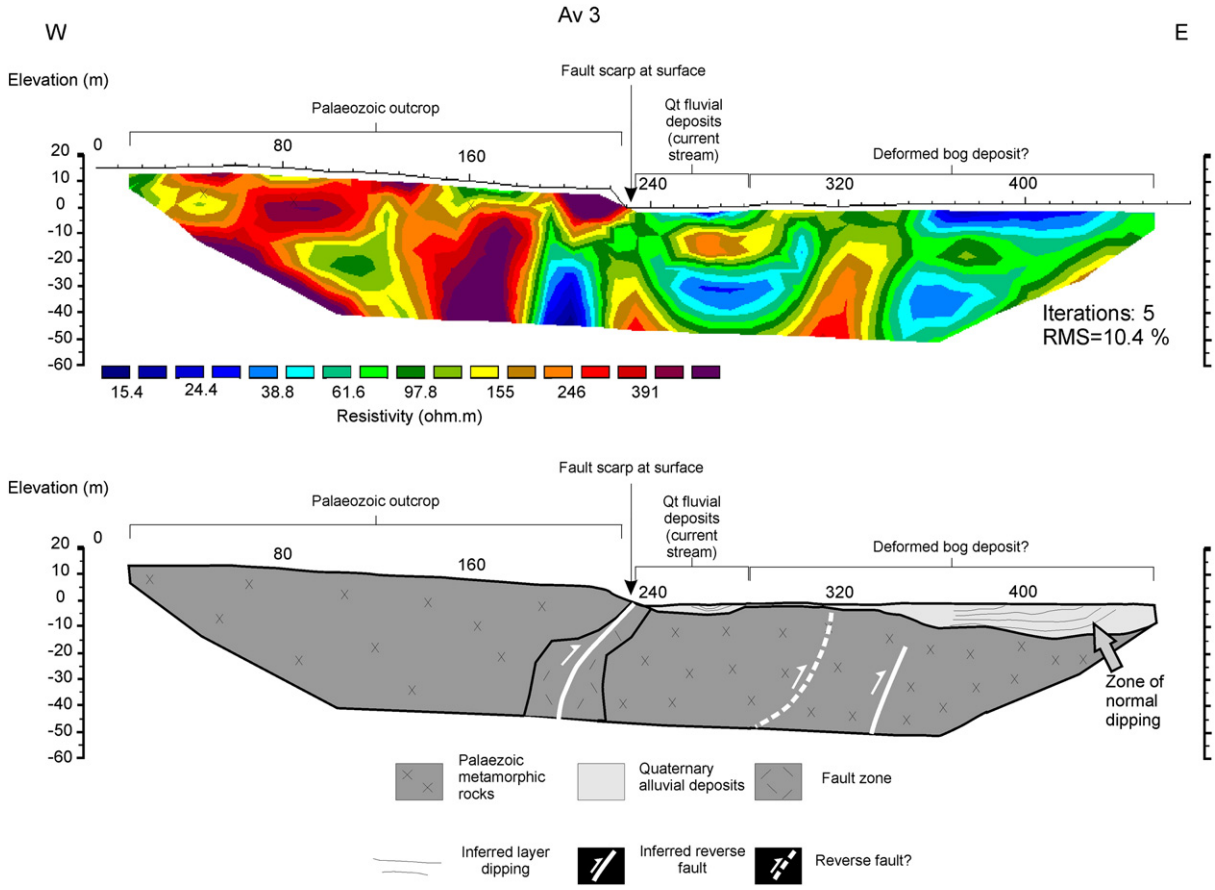

Fig. 10. Tomography of electrical resistivity AV3. a. Selected inverse model performed through the Los Avestruces Southern high. A dipole–dipole array was used with a unit electrode spacing of 10 m. (Smooth-constrained inversion with smoothing of model resistivity values). Maximum penetration depth was 50 m. b. Interpreted geological cross-section.

bog sediments. Furthermore, this is steeply bounded to the east by a lower resistivity area ($d \sim 390$ m), which on surface coincides with the vaulted NNE-trending bog zone. The larger resistivity zone is interpreted as a substratum high, uplifted by a west-dipping blind reverse fault (Fig. 9) which develops a subtle geomorphological expression at surface.

Finally, in the low resistivity zone that matches with the bog sediments, the presence of beds apparently dipping towards the east is tentatively interpreted. If this is confirmed, beds dipping opposite to their original slopes would strongly suggest tectonic tilting of the Pleistocene-Holocene infill.

The pattern shown by the AV3 profile (Fig. 10) agrees with that of AV2. It shows also a western zone with higher resistivity ($\rho > 100\ \Omega$ m, $0 < d < 230$ m) corresponding to the Palaeozoic outcrops of the southern high, and an eastern lower resistivity zone ($0 < \rho < 200\ \Omega$ m, 230 m $< d <$ 470 m) associated to the bog deposits. Between them there is a low resistivity (subvertical to west-dipping) conspicuous discontinuity. As in the AV2 profile, this is correlated with a fault scarp on surface and hence with the main reverse fault which uplifted the southern high.

The eastern zone (230 m $< d <$ 470 m) displays lower resistivity at shallow levels ($0 < \rho < 50\ \Omega$ m) which is consistent with the fine sediments of the Los Avestruces bog. However, at deeper levels and between 280 m and 320 m, there is a higher resistivity area (100 Ω m $< \rho <$ 250 Ω m) which extends into depth. This resistivity high is also interpreted as Palaeozoic substratum uplifted by a west-dipping blind reverse fault (Fig. 10).

5. Proposed kinematic model for the Los Avestruces deformation zone

The presence of *en echelon* structural elements in a deformation zone is not restricted only to strike–slip faulting (Sylvester, 1988), but from theoretical and experimental basis (see Sylvester, 1988 and Woodcock and Schubert, 1994) when occurring in narrow elongate zones usually indicate a lateral component of displacement along them.

The direction of the horizontal movement on the strike–slip fault zone is revealed by the stepping direction of the folds and/or thrusts: right-stepping folds or thrusts form in dextral slip; left-stepping folds of thrusts form in sinistral slip. Thus, from the geometry of the strain pattern in simple shear, it is possible to deduce the slip direction of the strike–slip fault zone (Sylvester, 1988).

In simple strike–slip shear zones, where there are no components of transpression or transtension, the axes of extension and shortening are at an angle of 45° to the principal shear zone (PSZ). The folds and thrust in these narrow zones form initially perpendicular to the axis of maximum shortening, and consequently, at an angle of 45° to the PSZ. If the deformation continues, the fold axis and the faults will rotate. Then, they will be at an angle $< 45°$ to the PSZ.

Transpression is considered as a transcurrent shear accompanied by horizontal shortening across the shear plane (Sanderson and Manchini, 1984) which is compensated by vertical thickening (Woodcock and Schubert, 1994). It means a coeval lateral displacement (simple shear) and shortening (pure shear). Thus, in a convergent or transpressive strike–slip zone, a component of shortening is imposed on the deformation zone.

An important feature of transpressive shear zones is that reverse displacements will tend to dominate over normal displacement. Therefore, in comparison with simple strike–slip or transtensive strike–slip zones, transpressive strike–slip zones will lead to the development of abundant reverse faults, such as thrusts and folds that are arranged en echelon.

Furthermore, transpression induces a horizontal strain ellipse with its long axis at a lower angle ($< 45°$) to the PSZ boundaries than in

simple strike–slip (Woodcock and Schubert, 1994). Here, the fold axis and the reverse faults will build up at lower angles to the PSZ.

The reactivation of pre-existing dipping faults, oblique to the present orogenic belt, would result in a contribution of strike–slip as well as vertical slip components. In the case of our study, as it could be appreciated from the tomographies of electrical resistivity, the pre-existing structures may correspond to extensional ones, related to the Triassic Cuyana basin. In a context of a compressional regime (like the Andean one) these structures would be reactivated as oblique reverse faults, forming a convergent or transpressional shear zone. A transpressional strike–slip zone can be characterized by an assemblage of associated contractional structures.

The Los Avestruces neotectonic deformation zone is composed by structural highs with a left-lateral arrangement and associated NNW to NNE-trending reverse faults (Figs. 2, 11a). On the basis of their en echelon arrangement, we interpret the strain field as characterized by a horizontal strain ellipse with its long axis (*X* axis in Fig. 2b) at an angle of <45° with respect to the principal shear zone (PSZ) boundaries (Fig. 11b) — (Sanderson and Manchini, 1984). Due to their contractional nature, they are interpreted as having developed under a transpressive regime. This kinematic model of the NW-trending Los Avestruces deformation zone is consistent not only with the kinematics of other NW major-scale structures of the region, such as the Barreal–Las Peñas belt, but also with the regional Late Cenozoic to present contractional geodynamic regime, which is governed by oblique convergence (Az 80°–85°) of the Nazca and the South American plates.

6. Discussion and conclusions

At the northwestern edge of the Barreal–Las Peñas belt, in the piedmont area of the El Naranjo and Ansilta ranges, some neotectonic and geomorphic features allow the recognition of the Los Avestruces Quaternary deformation zone. The main surface evidence of Quaternary deformation in this zone are given by i) uplifted and tilted Quaternary deposits, ii) piedmont scarps, iii) Quaternary covered highs with rectilinear NW to NNW and NNE boundaries and iv) a NNE vaulted zone affecting Quaternary bog deposits.

Furthermore, the electrical resistivity survey across the Los Avestruces deformation zone allowed the observation of different rock bodies in the subsurface. According to their distribution and the surface information it could be possible to interpret the presence of Quaternary alluvial deposits tilted against their original slope. It could also be possible to elucidate the geometry of the NNE, west-dipping reverse fault and the NNW west-dipping reverse fault which uplifted the southern and the central highs respectively. Additionally, the resistivity models are consistent with the subsurface deformation of the Los Avestruces bog deposits. Since the development of the bog is

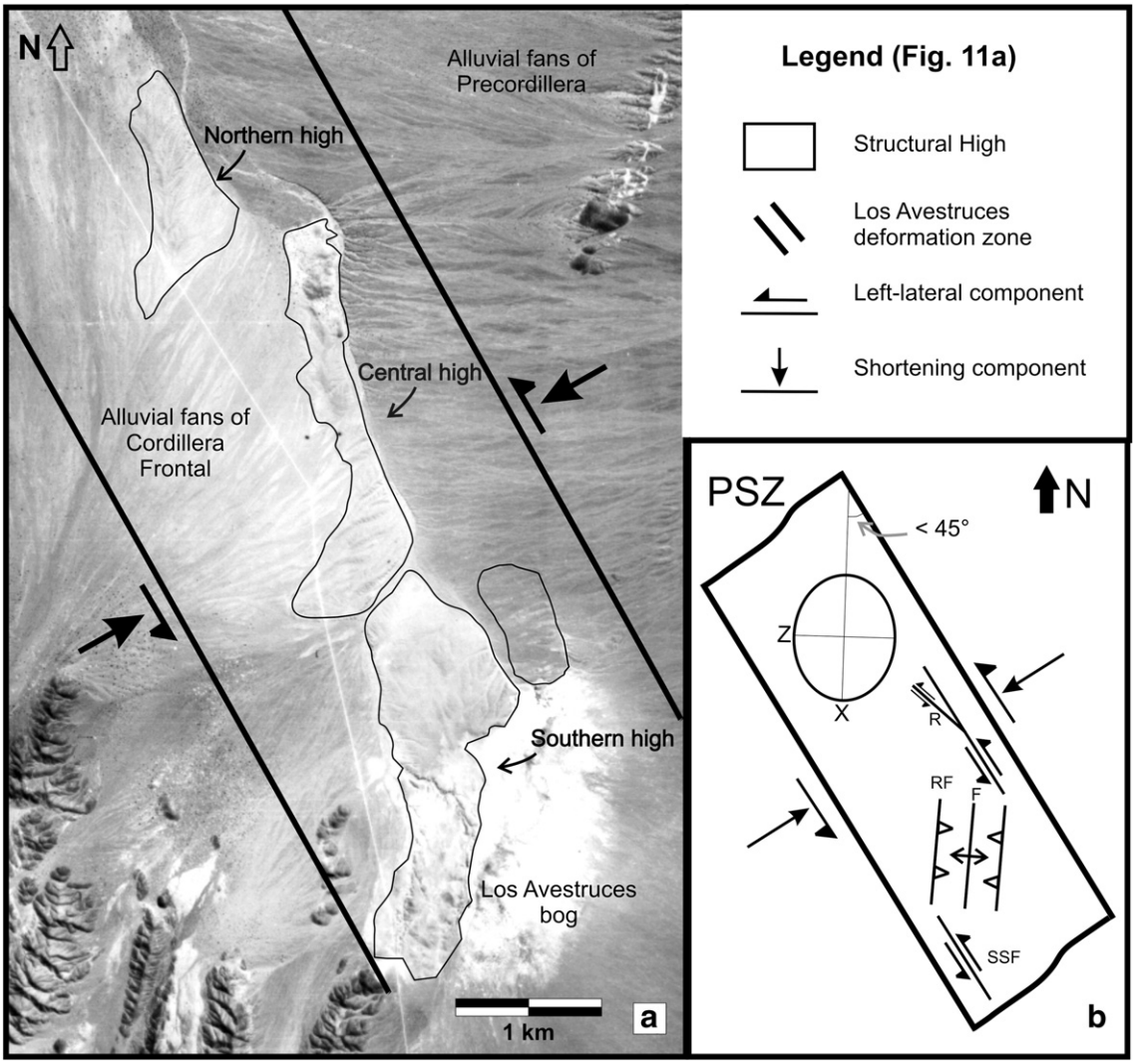

Fig. 11. a. Structural highs of the Los Avestruces deformation zone and Los Avestruces bog on an aerial view b. Kinematic model, under a transpressive regime, for the Los Avestruces deformation zone structures. PSZ: principal shear zone R: Riedel shear, RF: reverse fault, F: fold, and SSF: strike–slip fault.

interpreted as caused by the Quaternary uplift of the southern high and the consequent stream damming, it would be reasonable to interpret at least two Quaternary deformation events related to the Southern high uplift.

The Los Avestruces highs constitute a NW-trending neotectonic deformation zone hewed among the Palaeozoic substratum and the Pleistocene alluvial deposits of the Precordillera and the Cordillera Frontal piedmonts. Its left en echelon pattern and the angle (<45°) between the NW deformation zone and the NNW structural elements that constitute it, allow us to interpret the Los Avestruces deformation zone as a NW left-lateral transpressive shear zone (Terrizzano et al., 2007).

This pattern is repeated at different scales within the northern sector of the Precordillera Sur, examples of which are the Barreal–Las Peñas (Cortés et al., 2005a) and the Yalguaraz belts (Terrizzano and Cortés, 2008). These structural trends are not expected to be developed under the currently E–W (Az 80°–85°) Andean convergent regime. This situation is most likely caused by the direct interference between NNW–NW older structures (Triassic) and the current E–W Andean compressional regime. Indeed, the NW trend of the Los Avestruces deformation zone is consistent with the trends of all regional structures that, in turn, are consistent with the trends of extensional structures of the Cuyana basin. In such scenario, these structures would be reactivated during the Neogene to Quaternary (Cortés et al., 1997, 2008). In fact, as indicated by the AV1 electrical resistivity tomography the NNW reverse fault which cuts the Central high probably worked as a normal fault during the Triassic. This is interpreted as a previous extensional fault (associated to the development of the Triassic Cuyana basin) that has been reactivated and inverted in the Quaternary. We interpret this to be representative of the tectonic behaviour of a broader region characterized by Andean reactivation of Early Mesozoic structures.

Examples of shear zones, some of them transpressive ones, were actually largely described related to current convergence plate boundaries and reactivation of older structures. An interesting example was highlighted by Deffontaines et al. (1997) along the boundary between the Philippine Sea and Eurasian plates, in Taiwan. In this study, they described a series of NW-trending, left-lateral, Quaternary transfer fault zones, oblique to the trend of the Western Taiwan Foothills (NNE). There, the left-lateral shear should be induced by the ESE (N105°) compressional trends during Pleistocene times, and some of these (i.e. Sanyi and Pakua transfer fault zones) were interpreted as probably guided by weakness zones in the basement inherited from the extension of the Chinese passive margin. Furthermore, some of them show a transpressional mechanism of deformation (i.e. Chisham transfer fault zone). Other examples were provided along the Africa–Eurasia plate boundary, by Morel et al. (2000) at the northern High Atlas border (Morocco) and by Dhahri and Boukadi (2010) at the Atlas chain of Tunisia. These authors described a Neogene to Quaternary deformation event which was responsible for the inversion of Early Mesozoic extensional structures within the basement. As in the case of our study area, Morel et al. (2000) show a set of structures which were reactivated as transpressional fault systems. Furthermore, Morel and Meghraoui (1996) described along the same plate boundary the regional, 50–100 km wide, Goringe–Alboran–Tell transpressive system. The previously mentioned system is the consequence of the convergence between Africa and Eurasia and, in terms of size, it could be compared with the Barreal–Las Peñas belt.

Other examples were mentioned by Bonini and Sani (2000) at the Southern Apennine fold-and-thrust belt and by Claypool et al. (2002) in northern Fiordland, New Zealand. Bonini and Sani (2000) showed that some shear zones at the Apennine fold-and-thrust belt are controlled by pre-existing normal faults involved in the Pliocene sequences, which constituted weakness zones reactivated as reverse faults during Pliocene–Quaternary times. Claypool et al. (2002), concluded that, in Fiordland, pre-Cenozoic structures influenced and controlled the younger deformation patterns. They added that the orientations of the pre-Cenozoic structures with respect to the regional axes of shortening would explain the regional transpression. Finally, along the Andean margin farther north to our study zone, at the Eastern Cordillera of Colombia (between the boundary of the Nazca, South American and Caribbean plates), this kind of left-lateral transpressive fault system were cited by Acosta et al., 2004.

Acknowledgements

The authors would like to thank the reviewers of this article for their critical comments that significantly improved the final version. These studies were supported by grants from the Consejo Nacional de Investigaciones Científicas y Técnicas (CONICET) and the Universidad de Buenos Aires to José María Cortés (PIP no. 5422 and UBACyT X221) and Augusto Rapalini (PIP no. 5783 and UBACyT X262). The authors also thank Cecilia Spagnuolo and Ezequiel García Morabito for their help in the field.

References

Acosta, J., Lonergan, L., Coward, M.P., 2004. Oblique transpression in the western thrust front of the Colombian Eastern Cordillera. Journal of South American Earth Sciences 17, 181–194.

Azcuy, C.L., Caminos, R., 1987. Diastrofismo. In: Archangelsky, S. (Ed.), El Sistema Carbonífero en la República Argentina. Academia Nacional de Ciencias, Córdoba, pp. 239–251 (in Spanish).

Baldis, B., Beresi, M., Bordonaro, O., Vaca, A., 1982. Síntesis evolutiva de la Precordillera Argentina. 5ª Congreso Latinoamericano de Geología: Actas, 4, pp. 399–445 (in Spanish).

Bonini, M., Sani, F., 2000. Pliocene–Quaternary transpressional evolution of the Anzi-Calvello and Northern S. Arcangelo basins (Basilicata, Southern Apennines, Italy) as a consequence of deep-seated fault reactivation. Marine and Petroleum Geology 17, 909–927.

Caputo, R., Piscitelli, S., Oliveto, A., Rizzo, E., Lapenna, V., 2003. The use of electrical resistivity tomographies in active tectonics: examples from Tyrnavos Basin, Greece. Journal of Geodynamics 36, 19–35.

Caputo, R., Salviulo, L., Piscitelli, S., Loperte, A., 2007. Late Quaternary activity along the Scorciabuoi fault (Southern Italy) as inferred from electrical resistivity tomographies. Annals of Geophysics 50 (2), 213–223.

Claypool, A.L., Klepeis, K.A., Dockrill, B., Clarke, G.L., Zwingmann, H., Tulloch, A., 2002. Structure and kinematics of oblique continental convergence in northern Fiordland, New Zealand. Tectonophysics 359, 329–358.

Coggon, J.H., 1973. A comparison of IP electrode arrays. Geophysics 38, 202–221.

Colella, A., Lapenna, V., Rizzo, E., 2004. High-resolution imaging of the High Agri Valley Basin (Southern Italy) with electrical resistivity tomography. Tectonophysics 386, 29–40.

Cortés, J.M., 1998. Tectónica de desplazamiento de rumbo en el borde sur de la depresión de Yalguaraz, Mendoza, Argentina. Revista de la Asociación Geológica Argentina 53 (2), 147–157 (in Spanish).

Cortés, J. M., González Bonorino, G., Koukharsky, M. L., Pereyra, F. X., Brodtkorb, A. (1997). Hoja 3369-03, Yalguaraz, Provincias de San Juan y Mendoza. — 119 pp.; Servicio Geológico Minero Argentino (unpublished).

Cortés, J.M., Gonzalez Bonorino, G., Koukharsky, M.L., Brodkorb, A., Pereyra, F., 1999a. Hoja geológica 3369-09, Uspallata, provincia de Mendoza. Servicio Geológico Minero Argentino, Boletín 281 (in Spanish).

Cortés, J.M., Kleiman, L.E., Cortés, J.M., Kleiman, L.E., 1999b. La Orogenia Sanrafaélica en los Andes de Mendoza. 14° Congreso Geológico Argentino, Salta, Actas 1, 31 (in Spanish).

Cortés, J.M., Yamín, M.G., Pasini, M.M., 2005a. La Precordillera Sur, Provincias de Mendoza y San Juan. — 16º Congreso Geológico Argentino. La Plata, Actas 1, 395–402 (in Spanish).

Cortés, J.M., Casa, A., Pasini, M.M., Yamín, M.G., 2005b. Fajas de estructuras neotectónicas asociadas a rasgos paleotectónicos en Precordillera Sur y Cordillera Frontal (31º 30´– 33º 30´ LS). — 16º Congreso Geológico Argentino. La Plata, Actas 4, 463–466 (in Spanish).

Cortés, J.M., Japas, M.S., Pasini, M.M., 2008. El hemigraben triásico Paramillos, Precordillera Sur mendocina. — 17° Congreso Geológico Argentino. Jujuy 1279–1280 (in Spanish).

Costa, C.H., Machette, M., Dart, R., Bastías, H., Paredes, J., Perucca, L., Tello, G., Haller, K., 2000. Map and Database of Quaternary Faults and Folds in Argentina. U.S. Geological Survey Open-File Report 00-0108 (75 p).

Costa, C.H., Audemard, F.A., Becerra, F.H.R., Lavenu, A., Machette, M.N., París, G., 2006. An overview of the main Quaternary deformation of South America. Revista de la Asociación Geológica Argentina 61 (4), 461–479.

Dahlin, T., Zhou, B., 2004. A numerical comparison of 2D resistivity imaging with 10 electrode arrays. Geophysical Prospecting 52, 379–398.

Deffontaines, B., Lacombe, O., Angelier, J., Chu, H.T., Mouthereau, F., Lee, C.T., Deramond, J., Lee, J.F., Yu, M.S., Liew, P.M., 1997. Quaternary transfer faulting in the Taiwan Foothills: evidence from a multisource approach. Tectonophysics 274, 61–82.

Demanet, D., Renardy, F., Vanneste, K., Jongmas, D., Camelbeek, T., Megharaoui, M., 2001. The use of geophysical prospecting for imaging active faults in the Roer Graben, — Belgium. Geophysics 66 (1), 78–89.

Dewey, J.F., Lamb, S.H., 1992. Active tectonics of the Andes. Tectonophysics 205, 79–95.

Dhahri, F., Boukadi, N., 2010. The evolution of pre-existing structures during the tectonic inversion process of the Atlas chain of Tunisia. Journal of African Earth Sciences 56 (4/5), 139–149.

Fazzito, S.Y., Rapalini, A.E., Cortés, J.M., 2006. Tomografía geoeléctrica en zonas de fallas cuaternarias: dos ejemplos en la Precordillera centro-occidental de Mendoza. Revista de la Asociación Geológica Argentina. Serie D Publicación Especial N º 9, 41–47 (in Spanish).

Fazzito, S.Y., Rapalini, A.E., Cortés, J.M., Terrizzano, C.M., 2009. Characterization of Quaternary faults by electric resistivity tomography in the Andean Precordillera of Western Argentina. Journal of South American Earth Sciences 28, 217–228.

Fleta, J., Santanach, P., Martinez, P., Goula, X., Grellet, B., Masana, E., 2000. Geologic, geomorphologic and geophysic approaches for the paleoseismological analysis of the Amer fault (NE Spain). Workshop Proceedings of HAN2000: Evaluation of the Potential for Large Earthquakes in Regions of Present Day Low Seismic Activity in Europe. Han-sur-Lesse, Belgium, pp. 63–66.

Furqué, G., Cuerda, A., 1984. Estilos tectónicos de la Precordillera. — 9º Congreso geológico Argentino, San Carlos de Bariloche. Actas 2, 368–380 (in Spanish).

Giambiagi, L., Martínez, A., 2008. Permo-Triassic oblique extension in the Potrerillos–Uspallata area, western Argentina. Journal of South American Earth Sciences Vol. 26 (3), 252–260.

v. Gosen, W., 1995. Polyphase structural evolution of the southwestern Argentine Precordillera. Journal of South American Earth Sciences 8 (3/4), 377–404.

Japas, M.S., Kleiman, L.E., 2004. El ciclo Choiyoi en el bloque de San Rafael: de la orogénesis tardía a la relajación mecánica. Revista. Asociación Geologica Argentina, D, Publicación Especial 7, 89–100 (in Spanish).

Japas, M.A., Cortés, J.M., Pasini, M.M., 2008. Tectónica extensional triásica en el sector norte de la cuenca Cuyana: primeros datos cinemáticos. Revista de la Asociación Geológica Argentina 63 (2), 213–222 (in Spanish).

Kozlowski, E.E., Manceda, R., Ramos, V.A., 1993. Estructura. In: Ramos, V.A. (Ed.), Geología y recursos naturales de Mendoza: 12° Congreso Geológico Argentino y 2° Congreso de Exploración de HidrocarburosMendoza, Relatorio 1(18), pp. 235–256 (in Spanish).

Legarreta, L., Kokogian, D.A., Dellapé, D.A., 1993. Estructuración terciaria de la Cuenca Cuyana: ¿cuánto de inversión tectónica? Revista. Asociación Geologica Argentina 47 (1), 83–86 (in Spanish).

Lines, L.R., Treitel, S., 1984. Tutorial: a view of least-squares inversion and its application to geophysical problems. Geophysical Prospecting 32, 159–186.

Llambías, E.J., Kleiman, L.E., Salvarredi, J.A., 1993. El magmatismo gondwánico. In: Ramos, V.A. (Ed.), Geología y recursos naturales de Mendoza: 12º Congreso Geológico Argentino y 2º Congreso de Exploración de HidrocarburosMendoza, Relatorio 1, pp. 53–64 (in Spanish).

Loke, M.H., 1996–2009. Tutorial: 2-D and 3-D electrical imaging surveys. Geotomo Software.

Loke, M.H., 2001. Rapid 2-D resistivity and IP inversion using the least-squares method. Geoelectrical Imaging 2-D and 3-D. Geotomo Software.

Morel, J.-L., Meghraoui, M., 1996. Goringe–Alboran–Tell tectonic zone: a tranpression system along the Africa–Eurasia plate boundary. Geology 24 (8), 755–758.

Morel, J.-L., Zouine, E.-M., Andrieux, J., Faure-Muret, A., 2000. Déformations néogènes et quaternaires de la bordure nord haut atlasique (Maroc): rôle du socle et conséquences structurales (Neogene and Quaternary deformation of the northern High Atlas border (Morocco): role of the basement and structural consequences). Journal of African Earth Sciences 30 (1), 119–131.

Mpodozis, C., Kay, S.M., 1990. Provincias magmáticas ácidas y evolución tectónica de Gondwana: Andes chilenos (28°–31°S). Revista Geologica de Chile 17, 153–180 (in Spanish).

Nivière, B., Bruestle, A., Bertrand, G., Behermann, J., Gourry, J.C., 2008. Active tectonics of the south-eastern Upper Rhine Graben, Freiburg area (Germany). Quaternary Science Reviews 27, 541–555.

Ortiz, A., Zambrano, J., 1981. La provincial geológica de Precordillera Oriental. — 8º Congreso Geológico Argentino. Actas 3, 59–74 (in Spanish).

Ramos, V.A., 1988. The tectonics of the Central Andes: 30º to 33º S latitude. In: Clark, S., Burchfield, D. (Eds.), Processes in Continental Lithospheric Deformation: Geological Society of America, Special Paper, 218, pp. 31–54.

Ramos, V.A., Kay, S.M., 1991. Triassic rifting and associated basalts in the Cuyo basin, central Argentina. In: Harmon, R.S., Rapela, C.W. (Eds.), Andean Magmatism and Its Tectonic Setting: Geological Society of America, Special Paper, 265, pp. 79–91.

Ramos, E.D., Ramos, V.A., 1979. Los ciclos magmáticos de la República Argentina. — 7º Congreso Geológico Argentino. Actas 1, 771–786 (in Spanish).

Ramos, V.A., Jordan, T.E., Allmendinger, R.W., Kay, S.M., Cortés, J.M., Palma, M.A., 1984. Un terreno alóctono en la evolución Palaezoica de los Andes Centrales. — 9º Congreso Geológico Argentino, San Carlos de Bariloche. Actas 2, 84–106 (in Spanish).

Ramos, V.A., Jordan, T.E., Allmendinger, R.W., Mpodozis, C., Kay, S.M., Cortés, J.M., Palma, M.A., 1986. Palaezoic terranes of the central Argentine–Chilean Andes. Tectonics 6 (6), 855–880.

Rizzo, E., Colella, A., Lapenna, V., Piscitelli, S., 2004. High-resolution images of the fault-controlled high agri valley basin (Southern Italy) with deep and shallow electrical resistivity tomographies. Physics and Chemistry of the Earth 29, 321–327.

Sanderson, D.J., Manchini, W.R.D., 1984. Transpression. Journal of Structural Geology 6, 449–458.

Siame, L., 1998. Cosmonucleide Produit in situ (10Be) et Quantification de la Deformation Active dans les Andes Centrales. T. D. Université de Paris-Sud. U.F.R. Scientifique d' Orsay. (in French).

Siame, L., Sébrier, M., Bellier, O., Bourlés, D., Castaño, J.C., Araujo, M., 1997a. Geometry, segmentation and displacement rates of the El Tigre fault, San Juan Province (Argentina) from SPOT imagen analysis and 10Be datings. Annales Tectonicae Vol. XI (N.1).

Siame, L.L., Bourlés, D.L., Sébrier, M., Bellier, O., Castaño, J.C., Araujo, M., Pérez, M., Raisbeck, G.M., Yiou, F., 1997b. Cosmogenic dating ranging from 20 to 700 ka of series of alluvial fan surfaces affected by the El Tigre fault, Argentina. Geology 25 (11), 975–978.

Storz, H., Storz, W., Jacobs, F., 2000. Electrical resistivity tomography to investigate geological structures of the earth's upper crust. Geophysical Prospecting 48, 455–471.

Strelkov, E., Álvarez, L., 1984. Análisis estratigráfico y evolutivo de la cuenca triásica mendocina - sanjuanina. — 9º Congreso Geológico Argentino, San Carlos de Bariloche. Actas 3, 115–130 (in Spanish).

Sylvester, A.G., 1988. Strike–slip faults. Geological Society of America Bulletin 100, 1666–1703.

Telford, W.M., Geldart, L.P., Sheriff, R.E., 1990. Applied Geophysics, Second Edition. Cambridge University Press, Cambridge, UK. 790 pp.

Terrizzano, C.M., Cortés, J.M., 2008. Quaternary soft-linked fault systems highlighted through drainage anomalies in the northwestern Precordillera Sur (32ºS), Central Andes of Argentina. 7th International Symposium on Andean Geodynamics (ISAG). Nice, France, pp. 542–544 (Extended Abstracts).

Terrizzano, C.M., Fazzito, S.Y., Cortés, J.M., Rapalini, A.E., 2007. Quaternary transpressive zones in the Precordillera Sur, Argentina: a structural and geophysical approach. 20 Lateinamerika-Kolloquium Abstracts: 60. Kiel, Germany.

Uliana, M.A., Biddle, K.T., Cerdan, J., 1989. Mesozoic extension and the formation of Argentine sedimentary basins. In: Tankard, A.J., Balkwill, H.R. (Eds.), Extensional Tectonics and Stratigraphy of the North Atlantic Margins: American Association of Petroleum Geologists, Memoirs, 46, pp. 599–614.

Woodcock, N.H., Schubert, C., 1994. Continental strike–slip tectonics. In: Hancock, P.L. (Ed.), Continental Deformation. Pergamon Press, Oxford, pp. 251–263.

Yamín, M. G. (2007). Neotectónica del bloque Barreal, margen noroccidental de la Precordillera Sur. — PhD Thesis, University of Buenos Aires, 281 pp.